



**HAL**  
open science

## Artificial $\beta$ -defensin based on a minimal defensin template

Nikolinka Antcheva, Francesca Morgera, Luisa Creatti, Lisa Vaccari, Ulrike Pag, Sabrina Pacor, Yechiel Shai, Hans-Georg Sahl, Alessandro Tossi

► **To cite this version:**

Nikolinka Antcheva, Francesca Morgera, Luisa Creatti, Lisa Vaccari, Ulrike Pag, et al.. Artificial  $\beta$ -defensin based on a minimal defensin template. *Biochemical Journal*, 2009, 421 (3), pp.435-447. 10.1042/BJ20082242 . hal-00479131

**HAL Id: hal-00479131**

**<https://hal.science/hal-00479131>**

Submitted on 30 Apr 2010

**HAL** is a multi-disciplinary open access archive for the deposit and dissemination of scientific research documents, whether they are published or not. The documents may come from teaching and research institutions in France or abroad, or from public or private research centers.

L'archive ouverte pluridisciplinaire **HAL**, est destinée au dépôt et à la diffusion de documents scientifiques de niveau recherche, publiés ou non, émanant des établissements d'enseignement et de recherche français ou étrangers, des laboratoires publics ou privés.

## ARTIFICIAL $\beta$ -DEFENSIN BASED ON A MINIMAL DEFENSIN TEMPLATE

Nikolinka Antcheva<sup>\*</sup>, Francesca Morgera<sup>\*</sup>, Luisa Creatti<sup>\*</sup>, Lisa Vaccari<sup>§</sup>, Ulrike Pag<sup>†</sup>, Sabrina Pacor<sup>\*</sup>, Yecheil Shai<sup>‡</sup>, Hans-Georg Sahl<sup>†</sup> and Alessandro Tossi<sup>\*1</sup>

<sup>\*</sup>Department of Life Sciences, University of Trieste, 34127 Trieste, Italy, <sup>§</sup>ELETTRA Synchrotron Light Laboratory, Area Science Park, 34012 Basovizza, Trieste, Italy, <sup>†</sup>Institute for Medical Microbiology, Immunology and Parasitology, University of Bonn, 53105 Bonn, Germany, and

<sup>‡</sup>Department of Biological Chemistry, Weizmann Institute of Science, Rehovot 76100, Israel

<sup>1</sup>To whom correspondence should be addressed: Alessandro Tossi, Department of Life Sciences, University of Trieste, Giorgieri Street 1, 34127 Trieste, Italy. Tel.: +39 040 5583673; Fax: +39 040 5583691; E-mail: [atossi@units.it](mailto:atossi@units.it)

We have designed and chemically synthesised an artificial  $\beta$ -defensin based on a minimal template derived from the comparative analysis of over 80 naturally occurring sequences. This molecule has the disulfide-bridged,  $\beta$ -sheet core structure of natural  $\beta$ -defensins and shows a robust, salt-sensitive antimicrobial activity against bacteria and yeast, as well as a chemotactic activity against immature dendritic cells. An SAR study using two truncated fragments or a Cys $\rightarrow$ Ser point-mutated analogue, in which one or two of the three disulphide bridges were absent, indicated that altering the structure resulted in a different type of membrane interaction and a switch to different modes of action towards both microbial and host cells, and that covalent dimerisation could favour antimicrobial activity. Comparison of the structural, aggregational and biological activities of the artificial defensin with those of three human  $\beta$ -defensins and their primate orthologues provided useful information on how their mode of action may relate to specific structural features. (153 words)

**Short title:** ARTIFICIAL  $\beta$ -DEFENSIN

**Key words:**  $\beta$ -defensin, innate immunity, anti-microbial peptide, host defence peptide, chemotaxis.

**Abbreviations:** DMEM, dulbecco's modified Eagle's medium; FBS, foetal bovine serum; FS, forward scattering; hBD, *human*  $\beta$ -defensin; hcBD, *Hylobates concolor*  $\beta$ -defensin; JC-1, 5,5',6,6'-tetrachloro-1,1',3,3'-tetraethylbenzimidazolylcarbocyanine iodide; LUVs, large unilamellar vesicles; mfaBD, *Macaca fascicularis*  $\beta$ -defensin; MH, Mueller-Hinton; NHS, Normal human serum; OG, N-Octyl  $\beta$ -D-glucopyranoside; ONPG, o-nitrophenyl- $\beta$ -D-galactopyranoside; PBS, 10 mM sodium phosphate buffer pH7.4 with 150 mM NaCl; PC, phosphatidylcholine; PG, phosphatidylglycerol; PI, propidium iodide; SDS, sodium dodecyl sulphate; SEM, scanning electron microscopy; SPB, 10 mM sodium phosphate buffer pH7.4; SPPS, solid phase peptide synthesis; SPR, surface plasmon resonance; SS, side scattering; SUV, small unilamellar vesicle; TSB, tryptic soy broth.

## INTRODUCTION

Defensins are small, cationic host defence peptides involved in the innate immunity of organisms ranging from moulds and plants to vertebrate and invertebrate animals [1-3]. Structurally, they are amongst the smallest examples of autonomously folding polypeptides, displaying a characteristic triple-stranded, twisted, anti-parallel  $\beta$ -sheet scaffold [4-6] on which a short helix may be grafted, and whose formation seems to depend primarily on the presence of conserved disulphide bridges. Few residues are conserved in their sequences, apart from the cysteines involved in these bridges, and although the number, spacing and connectivity of the Cys residues varies in different defensin families, all determined structures conform quite closely to this characteristic fold [7-9]. It is a remarkable example of a small, conserved protein scaffold supporting an exceptional degree of sequence variation.

$\beta$ -defensins are defined by C<sup>1</sup>-C<sup>5</sup>, C<sup>2</sup>-C<sup>4</sup>, C<sup>3</sup>-C<sup>6</sup> connectivities, and have been identified in many vertebrate animals. Those involved in host defence are produced at epithelial surfaces and provide a multi-modal first line of defence against invading pathogens, which can involve direct inactivation of microbial cells and/or chemo attraction or stimulation of different types of host immune cells [10-14]. Each animal species possesses numerous paralogous defensin genes, which have arisen by multiple duplication events followed by bursts of sequence variation [15]. Orthologous genes in different species may then show different evolutionary patterns, ranging from positive selection for variation, to neutral evolution or conservation [16]. This is consistent with specific adaptations and specialisation within the innate immune or other responses, but what these are remains elusive, despite a vast literature on specific effects of  $\beta$ -defensins in different contexts. It has been difficult to correlate common or distinctive structural aspects of different  $\beta$ -defensin peptides with their distinct set of biological activities, and it doesn't help that some of these activities seem to persist even when the peptides' are linearized, fragmented or their structures otherwise altered [17-22].

The presence of a conserved structural scaffold supporting extensive sequence variation may be a leitmotif for antimicrobial peptides, which are at the interface between the host and pathogen and must thus respond to varying microbial biota. An extensively studied example are the amphipathic helical AMPs [23, 24], of which magainin is the type specimen [25]. The comparative sequence analysis of numerous such AMPs from different sources has allowed us in the past to describe this scaffold in terms of a sequence template, defining each position in terms of most frequent residues or residue types [23, 26], which was then used to guide the design of model peptides for structure-activity studies [27, 28]. Others have used alternative approaches, but in general, the use of simplified models for helical AMPs has been fundamental in the development of an articulated and widely accepted mechanism of action for these AMPs at the microbial membrane [29-31], which is often taken as the paradigm for other structural types also.

We have applied a similar approach to  $\beta$ -defensins and have carried out a comparative analysis of over eighty members of this family, taken from the AMSDb database of antimicrobial peptide sequences (<http://www.bbcm.units.it/~tossi/amsdb.html>). This allowed us to derive a simplified, artificial defensin sequence with characteristics common to many of the natural  $\beta$ -defensins. The synthetic peptide and its analogues are then used both for SAR studies, concerning activities on bacterial and host cells, and as benchmark molecules to help better understand the antimicrobial and immunomodulatory properties of natural peptides such as the human  $\beta$ -defensins 1 to 3 and their primate orthologues, in relation to their structure.

## EXPERIMENTAL

### Chemicals and reagents

Fmoc-protected amino acids, activators and resin for SPPS were from Applied Biotech Italy (Milan, Italy); Egg phosphatidylcholine (PC), Egg phosphatidylglycerol (PG), N-Octyl  $\beta$ -D-glucopyranoside (OG), bovine trypsin (EC 3.4.21.4), bovine chymotrypsin (EC 3.4.21.1), Igepal-HCl, CCR6 and ONPG were purchased from Sigma (Italy). DC-SIGN, CD29, CD11c were from Becton Dickinson (Italy). HLA-DR was from Immunotech (France). Recombinant human GM-CSF and recombinant human Interleukin 4 were from BioSource International (USA). Recombinant human Macrophage Inflammatory Protein-3 alpha (MIP-3 $\alpha$ ) was from Chemicon International (USA). FastDil and JC-1 were from Molecular Probes, (Invitrogen, Italy). BCA Protein Assay Reagent Kit was from PIERCE (Rockford, USA). Cholesterol (extra pure) was supplied by Merck (Darmstadt, Germany). Mueller-Hinton broth, Tryptic soy broth and Bacto-agar were obtained from Difco Laboratories (Detroit, USA). All other reagents and solvents were either synthesis or analytical grade.

### Sequence analysis

A sequence template for  $\beta$ -defensins was obtained by analysing the positional frequency of specific amino acids or amino acid types (charged, uncharged polar or hydrophobic) in 84 natural sequences belonging to human, primate, bovid, porcine, glires and avian species, aligned by the conserved cysteine residues [1]. For more conserved sequences (e.g. primate  $\beta$ -defensin 3), a limited subset was used to avoid bias. The artificial defensin sequence (tBD) was designed based on this template, also taking into account an appropriate charge distribution. Truncated peptides were then derived by simply removing N-terminal stretches to eliminate Cys<sup>1</sup> and then Cys<sup>2</sup> and converting the corresponding paired cysteines to Ser. A variant with a single point mutation was generated by converting Cys<sup>5</sup> to Ser, thus leaving one Cys unpaired. The mean per residue hydrophobicity of the peptides was determined using an amino acid hydrophobicity index scale developed previously as a consensus of numerous appropriately normalized published scales [23, 24].

### Peptide synthesis, folding and characterization

$\beta$ -defensin peptides were synthesized by Fmoc-solid phase peptide synthesis on a PE Biosystems Pioneer<sup>TM</sup> instrument with columns thermostated to 50 °C and loaded with 2-Chlorotrityl chloride resin, (substitution 0.2–25 meq/g), as described previously [7]. The quality of crude peptides was verified by ESI-MS (Sciex API I, Perkin Elmer) and then directly oxidatively folded (24 - 48h) in N<sub>2</sub>-saturated aqueous buffer (0.1 M NH<sub>4</sub>OAc, 2 mM EDTA, 1M guanidine. HCl, pH 7.5-8), containing Cys2/Cys pair (peptide/Cys2/Cys=1/10/100) as described [7]. Peptide concentrations were determined based on the molar extinction coefficients ( $\epsilon_{280}$ ) of Trp and Cys, using the ProtParam tool on the ExPASy server (<http://www.expasy.ch/tools/protparam.html>).

The disulfide connectivities in folded peptides were partly confirmed by limited digestion with bovine trypsin and/or chymotrypsin [peptide/enzyme ratio 20/1 (w/w)] at pH 5.5 to prevent disulfide exchange, followed by analytical RP-HPLC separation (Waters Symmetry 300Å, C18, 4.6 x 50 mm, 5  $\mu$ m analytical column) and ESI-MS determination of the fragments.

CD spectra were carried out on a Jasco J-715 spectropolarimeter (Jasco, Japan), using 2 mm path length quartz cells and peptide concentrations of 20  $\mu$ M, in 5 mM sodium phosphate buffer pH7, in the absence and presence of 10mM SDS. Electrophoresis of the peptides was performed in the absence of urea, under reducing and non-reducing conditions (with or without 2-mercaptoethanol as described previously [7]).

## Surface Plasmon Resonance on model membranes

Biosensor experiments were carried out with a BIAcore 3000 analytical system (BIAcore, Uppsala, Sweden) using an L1 sensor chip (BIAcore) whose surface consists of a dextran matrix modified with lipophilic compounds that capture SUVs thus permitting the retention of a bilayer structure as described previously [32, 33]. BSA (25  $\mu$ l, 0.1 mg/ $\mu$ l in PBS) was used as negative control to confirm complete coverage of non-specific binding sites. Peptide solutions in PBS (20-40  $\mu$ l, 0.3-45  $\mu$ M) were injected on the lipid surface at a flow rate of 5  $\mu$ l/min, followed by PBS alone and the peptide-lipid binding and dissociation events analyzed at six different peptide concentrations. In cases where the system reached a steady state during injection of the sample, the affinity constant was determined using kinetic models suitable for peptide-lipid interactions, using numerical integration analysis provided by the BIAevaluation software. A steady state reaction model was used, which considers the height of the signal to yield information on the binding affinity rather than the slopes, which were difficult to determine due to the shape of the curves.

## Transmission and ATR-FTIR

Transmission FTIR spectra (512 scans, spectral resolution 2  $\text{cm}^{-1}$ ) were collected with Vertex 70 Bruker spectrometer, using 2 mM peptide solutions in  $\text{D}_2\text{O}$  placed between  $\text{CaF}_2$  windows, spaced 25 microns apart in a dismountable liquid cell (Harrick Scientific Products, Inc.), after allowing the amide II band to shift from 1550 to 1460  $\text{cm}^{-1}$  to ensure complete deuterium exchange. Nonlinear least-square curve fitting with Gaussians bands was used to identify the components of the amide I band. Starting parameters for the fitting process were obtained by Second-derivative spectra (9-data-point Savitzky-Golay algorithm).

ATR-FTIR spectra (512 scans with a resolution of 2  $\text{cm}^{-1}$ ) were collected with the HORIZON<sup>TM</sup> multiple reflectance ATR accessory (Harrick Scientific Products, Inc.) mounted on a Bruker Vertex 70 instrument equipped with a Mid Band Mercury-Cadmium-Telluride detector (MCT D316). Lipid/peptide mixtures (1:20 w/w) were prepared by co-dissolving in a  $\text{MeOH}/\text{CHCl}_3$  (1:2) mixture on a clean Germanium crystal (50 mm x 10 mm x 2 mm), and then drying under a stream of  $\text{N}_2$ . The crystal was placed into a customized sealed ATR cell and hydrated by first increasing the relative humidity of the system, then introducing an excess of  $\text{D}_2\text{O}$  vapour into the sealed cell and following the H/D exchange process for 24 h by repeated measurement. The background was collected directly on a clean internal reflection element (IRE). Any contribution of water vapour to the absorbance spectra in the amide I peak region was corrected by spectral subtraction.

## Biological activity assays

### *Antimicrobial activity*

The bacteriostatic activity of the peptides was determined against *Escherichia coli* ML-35, *Pseudomonas aeruginosa* ATCC 27853, *Burkholderia cepacia* 6981 and 14273, *Staphylococcus aureus* 710A, *Staphylococcus simulans* 22 and a *Candida albicans* clinical isolate (c.i.) as minimum inhibitory concentrations (MIC), using the microdilution susceptibility test in 5% (v/v) TSB in SPB as described previously [26]. The bactericidal activity of peptides (time killing) was determined against *E. coli* ML-35 and *S. aureus* 710A ( $\sim 10^7$  CFU/ml in SPB incubated at 37°C) in the logarithmic phase and 8  $\mu$ M peptide concentration.

### *Effects on bacterial membrane integrity*

Permeabilization of the cytoplasmic membranes of *E. coli* ML-35 pYC by  $\beta$ -defensins, was evaluated by following the unmasking of cytoplasmic  $\beta$ -galactosidase activity using extracellular ONPG by standard methods [26]. The influence on uptake and retention of radioactive glutamate by *S. simulans*

( $\sim 10^6$  CFU/ml) in 25% (v/v) MH broth, was investigated as described previously [34]. Briefly cells were treated with radiolabeled L-[3H]glutamate (42 Ci/mmol, final concentration 10  $\mu$ Ci/ml), the sample divided into two aliquots, and one treated with 30  $\mu$ M tBD (10 times the MIC), while the other run as control. After 30 min the control was further subdivided into two aliquots, one of which received 30  $\mu$ M tBD to follow the effect on pre-accumulated amino acid. Samples were then filtered through cellulose acetate filters, washed twice, treated with unlabeled glutamate and dried before radioactivity determination, as previously described [34, 35].

To estimate the effect on the membrane potential of *S. simulans* 22, 1  $\mu$ Ci/ml of [3H]tetraphenylphosphonium bromide (TPP<sup>+</sup>; 26 Ci/mmol) was added to  $\sim 10^6$  CFU/ml cells in 25% (v/v) fresh MH broth. TPP<sup>+</sup> is a lipophilic cation which diffuses across the bacterial membrane in response to a trans-negative  $\Delta\psi$ . The culture was then treated with tBD at 10 times the MIC and samples were filtered and washed [34]. Counts were corrected for unspecific binding of [3H]TPP<sup>+</sup> by subtracting the radioactivity of 10% butanol treated cell aliquots. For calculation of the membrane potential ( $\Delta\psi$ ), TPP<sup>+</sup> concentrations were applied to the Nernst equation [ $\Delta\psi = (2.3 \times R \times T/F) \times \log (TPP^{+in}/TPP^{+out})$ ]. A mean  $\Delta\psi$  was calculated from a minimum of two independent determinations.

#### *Serum stability*

50  $\mu$ g of defensin peptides were incubated with 250  $\mu$ l of untreated human serum from healthy donors [25% (v/v) in PBS] at 37 °C for 24h. Aliquots of 25  $\mu$ l (5  $\mu$ g of peptide) were added to 65  $\mu$ l of cold 0.5% (v/v) of TFA in H<sub>2</sub>O at different time intervals: 0, 0.5, 1, 2, 4, 6 and 24h, kept on ice for 5 min and then centrifuged at 13000 rpm for another 5 min. The supernatants were injected into an LC-ESI-MS instrument [Amersham Pharmacia Biotech (Sweden) HPLC coupled to an ESQUIRE 4000 spectrometer, Bruker Daltonics (Germany)]. Components were separated using a Jupiter C18, 5  $\mu$ m, 300 Å, 2 X 150 mm micro-analytical column (Phenomenex, USA) with a linear gradient of 25% to 45% of acetonitrile in acidified water (0.05% TFA) in 30 min. The percentage of the intact peptide (P) was calculated from the area of the corresponding peak in the chromatogram ( $P = A_t/A_0 \times 100$ ), where  $A_t$  is the peak area of the peptide at any given time and  $A_0$  is the peak area at time zero.

#### *Cytotoxicity and chemotaxis assays*

Monocytes were prepared from buffy coat obtained from healthy donors and isolated by Histopaque® density gradient centrifugation. Immature DCs were then induced by treating monocytes with GM-CSF (25 ng/ml) and IL-4 (44 ng/ml) for 7 days (iDC7). A further aliquot of GM-CSF and IL-4 (2x) were added on the third day. iDC7 were phenotypically characterised using HLA-DR, CD11c, DC-SIGN, and CCR6 as markers, to confirm correct differentiation.

The hemolytic activity of peptides (at 10 or 100  $\mu$ M) was determined using 0.5% suspensions of human erythrocytes from healthy donors, in PBS, by monitoring the release of haemoglobin at 415 nm. 100% hemolysis was determined by addition of 0.2% Triton X-100. Cell viability of monocytes was determined by MTT standard procedures, after 1-24 h incubation with 1-16  $\mu$ M peptide in complete medium, and extensive washing with PBS. Apoptosis was assessed by either monitoring mitochondrial membrane depolarization, using the potentiometric JC-1 probe, according to the manufacturer's instructions (tech notes M34142, Molecular Probes), or by PI staining of EtOH fixed cells. Rehydrated cells were resuspended in staining solution (10  $\mu$ g/ml propidium iodide (PI), 0.05  $\mu$ g/ml fluorescein isothiocyanate (FITC) and 4  $\mu$ g/ml RNase in PBS) overnight before flow cytometric analysis. The percentage apoptotic (subG1) cells was determined using the Multicycle software (Beckman Coulter). All assays were carried out in triplicate and repeated at least three times. All flow cytometric measurements were carried out on a Cytomics FC 500 (Beckman Coulter) and data analysed with the WinMDI (J. Trotter, Scripps Research Institute, La Jolla, CA, U.S.A.) or Multicycle software. Data were subjected to computer-assisted ANOVA (Instat software, GraphPad Inc., San Diego, CA) followed by the Student–Newman–Keuls post test.

In vitro iDC migration was assessed in a Transwell cell culture chamber with 8.0  $\mu\text{m}$  pore size polycarbonate filters (Corning-Costar). Cells ( $10^6/\text{ml}$ ) were stained with FastDil dye (0.1 mM) for 20 min. at 37°C, thoroughly washed and resuspended in RPMI-1640, 1% BSA. 100 $\mu\text{l}$  suspension was added to the upper compartment, while the chemotactic stimuli, peptides (1  $\mu\text{M}$ ) or MIP-3 $\alpha$  (12.5 nM, positive control) were placed in the lower wells of the chamber. After 90 min. incubation, both migrated and transmigrating cells were quantified fluorimetrically at 530 nm on a Packard FluoroCount instrument. To specifically inhibit receptor-mediated chemotaxis, cells were pretreated with CCR6 antibody, at 0.5  $\mu\text{g}/10^5$  cells, for 30 min; neutralizing antibody, at 4  $\mu\text{g}/\text{ml}$ , was then also added to each lower compartment.

## RESULTS

### Defensin template

The frequency of different amino acid residues and residue types at each sequence position was determined for over 80  $\beta$ -defensins of mammalian and avian origin [1]. Although the peptides were of different sizes (36-50 residues), alignment was facilitated by the presence of 6 conserved Cys residues. The aligned sequences were quite variable (as qualitatively shown by the histogram in Figure 1A), so that apart from the cysteines very few positions are significantly conserved (Figure 1B). Taking into account moderately conserved residues (> 30% frequency at any given position) allows the definition of a template, as shown in Figure 1C. This was then used to design the artificial sequence tBD (template  $\beta$ -defensin), considering primarily the positional conservation of residue *types* (i.e. polar, hydrophobic or charged residue). Preference was in general given to the most common residue at any position but also took into account the necessity to achieve an appropriate cationicity, charge distribution, and hydrophobic/polar residue balance. Considering the most frequent charge in the natural peptides is +4, +6 or +7 (Figure 1F left), we chose a charge of +6 and kept the % hydrophobic residues within the most frequent range (26-30 %, Figure 1F right).

The most variable regions in natural  $\beta$ -defensins are located at the N- and C-termini. As shown by the topological diagram (Figure 1E) the N-termini may [6, 36] or may not [37] assume an  $\alpha$ -helical conformation of varying stability. In designing tBD, we have opted for a minimalist approach with a very short N-terminal sequence, and the peptide initiates with a pyroglutamic acid ( $\dot{E}$ ), as occurs in several bovid peptides, just 4 residues from Cys<sup>1</sup>. The C-terminal sequence was modelled on several human, murine, bovine and avian sequences. Figure 2 shows an alignment of tBD with selected natural  $\beta$ -defensins. Identity is highest with a subset of bovine sequences, but it is reasonable also with porcine, horse, human and murine peptides, while it shows less resemblance to other primate and avian sequences.

### Synthesis and characterisation

Linear tBD was synthesised by solid phase Fmoc-chemistry in good yields and over 95% purity, as confirmed by ESI-MS (not shown). Efficient folding to the correct structure was obtained in the presence of the free cysteine/cystine pair to allow bridge exchange, at slightly basic pH (7.5-8.0), and benefited from the high purity of the crude peptide. The major species, as determined by analytical RP-HPLC (supplementary material Figure S1), was partly confirmed to have the canonical  $\beta$ -defensin connectivities (Table 1) by ESI-MS of the fragments obtained by enzymatic digestion (Supplemental data Table S1).

A set of variants was obtained by truncating the peptide from the N-terminal, so as to systematically eliminate one then two disulphide bridges, [tBD(10-38) and tBD(16-38) in Table 1]. The loss of a cationic residue was balanced by introduction of a free terminal amine, so the overall charge is unvaried. A linear version of the shortest fragment was also prepared by alkylation of Cys residues with iodoacetamide. Replacing only Cys<sup>5</sup> with Ser led to tBD(Ser<sup>34</sup>) (Table 1), eliminating the C<sup>1</sup>-C<sup>5</sup> bridge, allowing for covalent dimerisation via intermolecular S-S bridging. The connectivities of Cys residues for all these molecules were analysed by limited proteolysis (Table S1), and while the

truncated fragments maintained the correct residual connectivities, the point mutated peptide did not, in line with what occurs also in natural defensin variants of this type [37]. tBD(Ser<sup>34</sup>) existed in partly separable monomeric and dimeric forms (Table S1).

Peptide structure was evaluated using both CD and FTIR spectroscopies in low salt buffer or in the presence of SDS micelles or PG multi-bilayers, which mimic a membrane environment. In aqueous solution, tBD shows a CD spectrum characteristic of a prevalently  $\beta$ -sheet structure with no apparent helical content (Fig. 3A), so it appears to assume the canonical defensin core structure devoid of an N-terminal helix. Removing one S-S connectivity in tBD(Ser<sup>34</sup>) has a destabilising effect, resulting in a strong random coil contribution. This is the case also for the truncated fragments, with little apparent  $\beta$ -sheet or  $\beta$ -hairpin content in aqueous medium, as well as the linearized fragment tBD(16-38)lin (not shown). In the presence of SDS micelles (Fig. 3B), the  $\beta$ -sheet structure of tBD becomes more pronounced, so that interaction with a membrane-like environment appears to have an additional stabilizing effect on the defensin core, whereas its mutated or truncated or linearized analogues remain prevalently disordered.

These results are confirmed by FTIR spectroscopy. In deuterated aqueous solution, tBD shows a well defined spectrum (Figure 4A) with components (see Figure 4C) characteristic of a  $\beta$ -sheet (shoulders at 1623 and 1670  $\text{cm}^{-1}$ ), with an estimated  $\beta$ -sheet content of about 40% and random coil of about 60% via curve fitting (see supplementary Figure S3). In the presence of a supported PG multi-bilayers (Figure 4B), ATR-FTIR indicates an increased conformational stability (55%  $\beta$ -sheet, 30% coil, see supplementary Figure S4). tBD(Ser<sup>34</sup>) and the truncated analogues instead result in transmission spectra in aqueous solution, and ATR spectra in the presence of supported PG multi-bilayer, that do not indicate a significant  $\beta$ -sheet content (Figure 4 and supplementary Figures S3 and S4). Furthermore, deuterium exchange for tBD in the presence of the supported PG multi-bilayer is significantly slower than that for tBD(Ser<sup>34</sup>) (Figure 4E) or the truncated analogues (not shown), indicating a tighter interaction with the model membrane.

Natural peptides such as human hBD2 have been proposed to form dimeric or higher order structures at high concentrations [4, 14] although this has not been experimentally confirmed. hBD3 has instead been observed by us and others to form aggregates at micromolar concentrations [6, 7] under non reducing conditions, using electrophoretic methods. A similar experiment was performed with tBD and its analogues as shown in Figure 3C, from which it appears that tBD remains monomeric. Two RP-HPLC fractions of tBD(Ser<sup>34</sup>), identified by mass spectrometry as respectively being prevalently dimeric (fraction 1) and prevalently monomeric (fraction 2) (Table S1), in fact both showed the presence of the dimeric form, with monomer present only in fraction 2. This may indicate an equilibrium favouring the dimeric form, which is quite stable as indicated by the difficulty in eliminating it completely even under reducing conditions (Figure 3C).

### Biological activities

A first evaluation of the cytotoxic activity for tBD and its analogues on microbial cells was based on their minimum inhibitory concentrations (Table 2). MIC determinations were carried out in 5% (v/v) TSB or Sabouraud broth in SPB, as defensins are known to be generally quite sensitive to salt and medium conditions. Under these conditions tBD shows a robust and broad spectrum activity against all tested micro-organisms (MIC = 2-4  $\mu\text{M}$ ), excepting *B. cepacia* which is well known to be resistant to AMPs [38, 39]. The antimicrobial behaviour of tBD therefore appears to be entirely in line with that of natural  $\beta$ -defensins (Table 3).

tBD(Ser<sup>34</sup>) showed a reduced activity for the monomer enriched fraction 2 but not for the predominantly dimeric fraction 1. The truncated peptide tBD(10-38) actually showed increased antimicrobial activity under these conditions, and even the shorter fragment tBD(16-38), with only one disulphide, displayed relatively low MIC values. Only complete linearization of this fragment significantly reduced activity. It should be noted that all peptides have a charge of +6, so that the initial electrostatic interaction with the microbial membranes should be similar. The mean residue hydrophobicity of tBD, tBD(Ser<sup>34</sup>) and tBD(10-38) are also quite similar whereas it is reduced in the smaller truncated peptide, which may explain its lower activity (Table 1).

The fact that abrogating the canonical defensin conformation, as occurs in tBD(10-38), seems to increase the *in vitro* antimicrobial potency suggests that the latter peptide may be acting via a different mechanism. To test this hypothesis, the susceptibility of MIC values to medium conditions was analysed (Figure 5). As expected for a defensin, the activity of tBD against bacteria and yeast was significantly reduced at higher medium concentrations, while that of tBD(10-38) was notably less affected. This is consistent with different mechanisms of action.

Killing kinetics experiments (Figure 6A) against *E. coli* and *S. aureus* showed a two log drop in viability for both bacteria within one hour of exposure to 8  $\mu$ M tBD (2- 4  $\times$  MIC), under low salt conditions, while complete inactivation required longer periods. However, at higher peptide concentrations (30  $\mu$ M), the killing capacity towards *S. simulans* was rapid and total, even at 25% (v/v) MH medium (Figure 7A). tBD thus has a cidal rather than just bacteriostatic antimicrobial activity.

The bactericidal activity of natural  $\beta$ -defensins is proposed to depend, at least in part, on their capacity to somehow compromise the microbial membrane, leading to leakage of cell content and consequent, or subsequent, inactivation [14, 15]. The capacity of tBD and its variant or truncated fragments to permeabilize the cytoplasmic membrane of *E. coli* was tested on the  $\beta$ -galactosidase constitutive ML35 pYC strain, under low salt conditions, by following the hydrolysis of the impermeant extracellular chromogenic substrate ONPG (Figure 6B). All tBD derived peptides resulted in cytoplasmic membrane permeabilisation, albeit with slower kinetics than the control helical lytic AMP P(19/5)B [28]. Unlike tBD and tBD(Ser<sup>34</sup>), the truncated fragments show convex curves, with a considerable lag-time for the shorter tBD(16-38), after which significant permeabilization occurs. This further suggests that the truncated fragments may have different modes of action to tBD, possibly causing more membrane damage in the long term.

To evaluate the stability of tBD and its analogues to the proteolytic effect of serum, aliquots were incubated with 25% (v/v) human serum for different times and then analysed by LC-MS for peptide integrity (Figure 6 C). tBD was quite stable (100% intact even after 24h incubation). The truncated analogues with two [tBD (10-38)] or one [tBD(16-38)] disulfide-bridged were instead rapidly degraded, with respectively only 30% and 10 % integral peptide detected after 4h of incubation, and full degradation after 24h. The serum stability of tBD (Ser<sup>34</sup>), which is primarily dimeric, was difficult to assess, as in the presence of serum it resulted in multiple HPLC peaks with very weak MS signals (not shown). A possible explanation is that it interacts strongly with serum components in a manner that segregates it.

The cytotoxic activity of tBD was assessed by monitoring PI permeabilization of monocytes as well as hemolytic activity. As for natural defensins, treatment of erythrocytes with peptide concentrations well above the MIC (up to 100  $\mu$ M) resulted in little damage (Table 2). The truncated variants tBD(10-38) had a comparable hemolytic activity to tBD under similar conditions, while curiously, the dimeric tBD(Ser<sup>34</sup>) peptide showed a significant hemolytic effect. Permeabilisation of monocytes to PI, and the MTT viability assay performed on monocytes and iDC7 at peptide concentrations up to 4  $\mu$ M also indicated a lack of cytotoxicity (not shown).

### Antimicrobial mode of action

To probe the mode of action of tBD, a series of assays were carried out under identical conditions, to correlate bactericidal and membrane effects (Figure 7). *Staphylococcus simulans* was used as the reference strain, as a large body of data already exists for several other AMPs [40]. At 10 times its MIC value (30  $\mu$ M) in 25% (v/v) MH medium, complete inactivation of bacteria occurred within 20 minutes (Figure 7A & B), and concurrent membrane depolarization was also observed ( $\sim$  20 mV decrease within 10 min, Figure 7C), as assessed by the distribution of the lipophilic cation TPP<sup>+</sup> inside and outside cells. This effect is however considerably smaller than for known pore-forming agents such as nisin [35] which completely depolarise cells. The anionic potential-sensitive fluorescence dye bis-(1,3-dibutylbarbituric acid)trimethine oxonol, also indicated a rapid partial depolarization (not shown). Treatment of cells with the peptide completely abrogates their capacity to actively accumulate tritiated glutamate (Figure 7D), and similar results were obtained for incorporation of <sup>3</sup>H-uridine, <sup>3</sup>H-

glucosamine,  $^{14}\text{C}$ -thymidine and  $^{14}\text{C}$ -proline (not shown), possibly because of insufficient energization of the membrane. When tBD was added to cells previously incubated with  $^3\text{H}$ -Glu for 30 min (Figure 7D, arrow), uptake ceased immediately, but there was only partial efflux of the accumulated amino acid. This, together with the incomplete depolarization, clearly argues against only a straightforward membranolytic mechanism occurring, resulting in a complete loss of its barrier function; it rather suggests that tBD may also act through disruption of the functional organization of membrane bound complexes such as the respiratory chains, ATPase and solute transport systems.

### Binding affinity to lipid bilayers - a steady-state affinity model

The interaction of tBD and its truncated fragments with model biological membranes was probed using surface plasmon resonance. Sensograms for binding to PC/cholesterol (10/1 w/w) or PE:PG (7:3 w/w) bilayers are shown in Figure 8. The response unit (RU) signal intensity in all cases increased as a function of the peptides concentration, indicating the capacity of all peptides to bind with the lipid bilayers. Sensograms for binding to anionic PE:PG bilayers (Figure 8B and D) showed a similar type of interaction for all the peptides at lower concentrations ( $< 4 \mu\text{M}$ ), while tBD showed markedly higher response levels compared to those of either tBD(10-38) or tBD(16-38) (not shown) at higher concentration ( $> 7 \mu\text{M}$ ). Moreover, dissociation of tBD from these bilayers was incomplete at these higher concentrations (Figure 8B), while complete dissociation was observed for truncated peptide at all concentrations (Figure 8D). A similar behaviour was observed with neutral PC/cholesterol bilayers (Figure 8A, C), but with less differentiated response levels. In general, the truncated peptides showed a relatively flat relationship of the equilibrium binding response with concentrations above  $1 \mu\text{M}$  peptide, while tBD shows a linear increase up to the highest concentrations (Figure 8, panels E & F).

Truncated peptides are reversibly binding to the zwitterionic or anionic membranes, and as the system reached binding equilibrium during the injection of the sample it was possible to calculate the affinity constants (the ratio of the association and dissociation rate constants, i.e.  $K_A = k_a/k_d$ ) from the equilibrium binding response curves shown in Figure 8E & F. Using a steady-state affinity model values of  $K_A = 1 \times 10^6$  and  $5 \times 10^6 \text{ M}^{-1}$  were determined for tBD(10-38) and tBD(16-38), respectively. The affinity constant for tBD could not be obtained because its binding is irreversible. These results further suggest that the parental and truncated peptides have different modes of membrane interaction, which may lead to different types of insertion and/or permeabilization/translocation events.

### tBD as a benchmark peptide for natural $\beta$ -defensins

We have compared the structural characteristics and antimicrobial activities of tBD with that of the three human defensins hBD1-3, and three primate orthologues, respectively from macaque (*mfaBD1-2*) and gibbon (*hcBD3*) [7, 15, 41, 42]. As shown in Table 3, the salt-sensitive antimicrobial activity of tBD compares quite favourably with that of the natural peptides. It is more potent than all the  $\beta$ -defensin 1 and 2 orthologues, indicating that the  $\beta$ -sheet platform is sufficient for a robust and broad-spectrum bacteriostatic activity, and that the presence of an extended N-terminal segment or helix does not seem to be essential. Only the  $\beta$ -defensin 3 orthologues show significantly lower MIC values; but their elevated cationicity may play a key role in determining this potency.

Comparing the CD spectra of tBD (Figure 3) and hBD2 [15] indicates an important  $\beta$ -sheet contribution for both in aqueous solution, and the contribution from a stable helical segment in hBD2, that is absent in tBD, becomes more apparent. In the presence of SDS micelles, the spectra of both peptides become more intense so that interaction with a lipidic environment may stabilise the  $\beta$ -sheet structure. Significantly, hBD2 shows a comparable stability to serum degradation (98% intact peptide after 24 hrs incubation, see Fig. 6C) to tBD. This indicates that stability to proteolysis is favoured by overall scaffold stability.

Conversely, the CD spectra for *mfaBD2*, hBD3 and *hcBD3* in aqueous solution [15], by comparison to the tBD spectrum, have a considerably greater contribution from unordered conformations. The explanation, for hBD3 for example, is that the presence of wide loops and a long

and relatively disordered N-terminal stretch dominates over the contribution of the relatively few residues forming the central  $\beta$ -sheet core [6]. A significant structural rearrangement seems to occur in the presence of a lipidic environment, with likely stabilisation of both the core and the formation of a long helical N-terminal segment for hBD3 in particular [43].

Comparison of the behaviour of tBD and its covalently dimerized analogue tBD(Ser<sup>34</sup>) with the natural peptides in PAGE experiments also allowed to better define their aggregation behaviour. tBD clearly behaves as a monomer in non-reducing conditions (Figure 3C lanes 3), and tBD(Ser<sup>34</sup>) prevalently as a dimer in fraction 1 and as a monomer in fraction 2 (Figure 3C lanes 5 & 7). It should be noted that due to the compact size, disulphide-bridge stabilised structure and relatively high cationicity, shielding by SDS is likely to be incomplete, so that the peptides travel with an apparent mass that is somewhat higher than expected. By comparison, hBD2 seems to be in equilibrium between monomeric and dimeric forms (Figure 3C lane 11), while its macaque orthologue behaves as a monomer under these conditions (Figure 3C lane 9). hBD3 clearly aggregates into a multimer (Figure 3C lane 15), despite its high charge, as also reported by Schibli et al. [6, 9]. *hcBD3* instead cannot do this, as it lacks a critical intramolecular salt-bridge that locally reduces cationicity [7]. hBD3 is in fact proposed to dimerize via electrostatic interactions between Glu28 in one molecule and with Lys32 on another, and vice versa. This however requires a local decrease in charge density [6], which occurs via intramolecular salt-bridging involving Glu27 and Arg17 (the relevant residues are shown in italics in Fig. 2). We have reported that in *hcBD3* the Arg17 to Trp mutation does not allow this and prevents it from oligomerizing [7], as observed in the PAGE experiments (Fig. 3C).

The looser structure of hBD3 in aqueous solution correlates with an increased susceptibility to degradation in serum (Fig. 6C, only 60% integrity after 4 hrs incubation), which however is still incomplete after 24h (50% integral peptide remaining). An explanation could be that while the less stable scaffold favours degradation, oligomerization shields some of the peptide subunits. Degradation seemed initiate at the C-terminus (-K, -KK, -RKK), as was detected by LC-MS, so is likely mediated by a carboxypeptidase (data not shown).

To obtain further insight into the mode of action of the natural peptides, the kinetics of bacterial inactivation of hBD2 and hBD3 were compared to that of tBD. Both hBD2 and hBD3 were considerably faster at inactivating the Gram-negative bacterium (supplementary Figure S2A) than the Gram positive one (supplementary Figure S2B), whereas tBD showed a comparable slower killing kinetics against both. This supports the proposal that the  $\beta$ -sheet core is sufficient for a basal antimicrobial activity while the added structural features (e.g. increased cationicity or presence of stable or inducible N-terminal helical stretches) further modulate it [43].

The human defensins hBD1 and in particular hBD2, have been reported to induce chemotaxis of immature dendritic cells (iDC), via the CCR6 receptor, which responds to the chemokine MIP-3 $\alpha$  [11-14]. We confirmed this effect for hBD2, albeit at a concentration (1  $\mu$ M) that is 100 fold higher than the native chemokine, consistent with literature results [11, 13]. A statistically significant increase in cell mobility of about 20% above spontaneous migration was observed, in line with about 20-50% of cells being positive for membrane exposed CCR6 (as determined using anti-CCR6 monoclonal antibody, not shown). Chemotaxis induced by tBD compared favourably to that induced by the human peptide hBD2 but curiously, so did that of the truncated and destructured peptide tBD(10-38) (Figure 9A). However, while CCR6 neutralising antibody was effective in reducing chemotaxis of iDC by both hBD2 and tBD, as with the endogenous chemokine MIP-3 $\alpha$ , it did not affect chemotaxis by the truncated peptide. This may indicate the presence of alternative chemotaxis mechanisms [44].

To further probe the activity of these peptides on iDC and their precursors, their effect on the mitochondrial membrane potential, assessed using the JC-1 probe, and that on the cell cycle, assessed via PI staining of fixed cells, were determined by flow cytometry, at the same concentration as used in chemotaxis experiments (1  $\mu$ M). As shown in Figure 9B, tBD and hBD2 had a relatively limited effect in both assays, while the truncated peptide tBD(10-38) caused a more significant mitochondrial depolarization ( $\Delta\Psi_m$ ) and a parallel increase in the percent of sub G1 cells ( $\sim$  10%), which may indicate an incipient apoptotic damage to the cells even at this low concentration. Globally, these results would seem to indicate that the truncated peptide has a different biological effect than tBD or hBD2 with respect to this type of host cells.

## DISCUSSION

We have designed, synthesised and characterised an artificial  $\beta$ -defensin, using features from the primary structures of numerous natural peptides. It should be underlined that only a subset of these have been characterised for biological activities, but it is assumed that they all play some role in host defence.  $\beta$ -defensin-like sequences from genomic studies, which may have different roles, were not used. Our designed molecule shows all the hall-mark features of characterized natural peptides, including a stable  $\beta$ -sheet core, a robust, broad-spectrum antimicrobial activity under low salt/low medium conditions, and the capacity to chemoattract immature dendritic cells. Exposure of bacterial cells to this peptide, even for brief periods, resulted in the halting of metabolic processes and bacterial killing, in a salt- and concentration-dependent manner.

Permeabilisation of the bacterial membrane was also observed, but penetration of impermeant substrates into the cytoplasm was slow, as previously reported also for natural  $\beta$ -defensins [15, 45], and only partial efflux of accumulated metabolites and incomplete depolarisation of the cytoplasmic membrane was observed. Supposing a membranolytic mechanisms for the defensin peptides, there is some incongruity between these rather slow and incomplete effects on membrane integrity and the fact that killing ensues after a quite brief exposure to the peptide. This could on one hand indicate that bacterial inactivation is not strictly dependent on membrane compromising. On the other, it could also be explained by a delayed membrane effect, due to the persistence of the peptide in membranes even after extensive washing, consistent with the partly irreversible nature of the interaction with model membranes, as indicated by SPR studies.

We have interfered with the well-defined structure of tBD, by either replacing only one of the conserved cysteines or removing entire sections containing Cys residues, while not affecting the overall charge. The single cysteine substitution causes a rearrangement of disulphide bridging and significantly destabilises the peptide's secondary structure, as observed with both CD and FTIR spectroscopies. Both a human polymorphic peptide, hBD1(Ser<sup>35</sup>), and a mouse variant, mBD8(Tyr<sup>5</sup>), with only 5 cysteines have been reported [20, 37]. The human peptide, like tBD(Ser<sup>34</sup>) shows an apparent rearrangement of the canonical connectivities, without significant loss of antimicrobial activity, and the mouse peptide, like tBD(S<sup>34</sup>), showed an increased antimicrobial activity when covalently dimerised. Removal of 2 cysteine residues along with part of the N-terminal region, in tBD(10-38) completely abrogated the canonical defensin conformation, irrespective of the environment. In agreement with literature reports for truncated natural defensin analogs [9, 18, 19, 21, 46], the *in vitro* antimicrobial activity of truncated tBD peptides endured, but with an apparent shift to a different mode of action. The integral defensin acts in a salt-sensitive manner, but interacts more irreversibly with biological membranes, as indicated by both SPR experiments, and slower deuterium exchange in ATR-FTIR experiments, using supported membrane multi-bilayers, and this leads to bacterial inactivation without rapid or massive membrane lysis. We have recently proposed that part of the antimicrobial mechanism for AMPs might derive from their capacity to disrupt the functional organization of membrane bound complexes, such as the respiratory chains and transport or cell wall assembly systems - a cidal mode of action called the "sand-in-a-gearbox" mechanism [34], and this may apply to tBD as well as natural  $\beta$ -defensins. The truncated peptides instead may act by a less salt-sensitive, reversible, possibly carpet-like and more lytic mechanism [30].

When the structural characteristics and antimicrobial activities of tBD were compared to those of several human and primate defensins, it confirmed its usefulness as a benchmark molecule. Of all the natural peptides, only hBD2 appeared to have a similarly well-formed  $\beta$ -sheet core structure, with an added stable helical component [4, 6, 47] in aqueous buffer. The other natural defensins seem to have less defined structures in bulk solution, although an increased structuring is induced by interaction with a lipid-like environment. The defensin scaffold may thus be dynamic, extending or reducing the  $\beta$ -sheet core and the attached N-terminal helical segment according to the supported sequence and

environment [43]. Judging from the robust and broad-spectrum activity of tBD, the  $\beta$ -sheet core is sufficient for a basal antimicrobial action, whereas the added structural features of the natural peptides (helical stretch, increased cationicity, etc.) further modulate it, for example altering potency, killing kinetics and salt sensitivity. It also appears that specific features in the primary structures of the natural defensins mediate their differential tendencies to oligomerise, whereas these are absent in tBD. Mode-of-action studies however argue against a straightforward membranolytic mechanism for bacterial killing but rather may be due to a disruption of the functional organization of membrane bound protein complexes. Recent studies using hBD3 have brought us to a similar conclusion for this natural defensin, and led us to propose that its antibiotic activity is based on interference with the organisation over space and time of membrane-bound protein machineries such as the electron transport chain and, in particular, the cell wall biosynthesis complex, rather than on formation of membrane lesions [48].

The presence of a stable  $\beta$ -sheet scaffold in aqueous solution is also important for serum stability *in vitro*. Thus, tBD and the human defensin hBD2 remained intact after 24h of incubation; hBD3, which has more disordered N- and C-termini [6], was only 50% intact, and truncated and disordered analogues of tBD were completely degraded. This is in line with an increased susceptibility of  $\alpha$ -defensins also to an extracellular proteinase, when the structure was altered by disrupting the disulphide array [49].

A comparison of iDC chemotaxis induced by hBD2, tBD and the truncated peptide tBD(10-38) was also quite revealing. tBD has a comparable effect to the human peptide, and also appears to act via CCR6, as indicated by its abrogation in the presence of anti-CCR6 antibody. This would seem to indicate that interaction with CCR6 does not depend on specific structural features of hBD2, such as the stable N-terminal helix, but rather on the generic defensin  $\beta$ -sheet platform, as present in tBD and other defensins. This is in line with the fact that human and mouse BD1, which are quite different in sequence to hBD2, also induce iDC chemotaxis [19, 50]. One could speculate that this may occur via a non-canonical interaction with the receptor that may depend on the capacity of these peptides to interact with the membrane around it rather than to the receptor binding site. Membrane accumulation of defensins in host-cells could in this way lead to productive interactions with membrane bound complexes, at non-toxic concentrations.

The fact that the truncated peptide tBD(10-38) also causes chemotaxis while not responding to CCR6 neutralizing antibody suggests that this effect can also be induced by membrane-active peptides in a manner not dependent on CCR6, in line with recent reports [44]. This may relate to a different type of membrane interaction, as indicated by SPR experiments, and may be pertinent to the observation by others also, that compromising the structure of defensins does not necessarily remove chemotactic activity [51].

The study of defensins is in general complicated by the fact that the number of reported antimicrobial and immunomodulatory activities *in vitro*, which may or may not be biologically relevant, is continually increasing, but so are reports of these activities persisting even when the canonical defensin structure is dismantled by linearization or fragmentation [17, 18, 20-22, 51]. It seems odd that a ubiquitous and evolutionarily conserved scaffold could be so easily dispensed with, even if it is known to support quite extensive sequence variation. With tBD we have found sequence conditions for ensuring formation of a quite stable, monomeric form of the scaffold and related this to its mode of antimicrobial and chemotactic action, which may be generally representative of that of the natural peptides. We have further shown that while altering the structure does not necessarily abolish antimicrobial or chemotactic activity *in vitro*, it likely results in a shift to different modes-of-action. Numerous highly simplified artificial AMPs, and even peptidomimetics, have been designed in which a suitable distribution of cationic and hydrophobic residues results in a potent biological activity *in vitro* [23, 40, 52]. It is therefore not surprising that the primary structure of defensins, which evidently shows this distribution, should result in such activities even in the absence of higher structural organisation. Whether this occurs by the same mechanisms, or is biologically meaningful, is another question. In other words, one can learn lessons from the evolutionarily selected features of naturally occurring peptides that can help in the design of novel AMPs with useful properties, but too much tampering may lead to ambiguous results. The observation of similar functions for HDPs and derived analogues should not be taken at face value, and the underlying mechanisms should be probed using a

number of complementary biological and biophysical methods, before drawing conclusions. We trust that tBD can in this respect be a useful benchmark for studying defensins and their analogues.

*This work was carried out within FVG regional project R3A2 and PRIN. Project (2005051341\_005). N. Antcheva gratefully acknowledges support from the EU 6<sup>th</sup> framework project ET-PA (COOP-CT-2005-018191).*

## REFERENCES

- 1 Antcheva, N., Zelezetsky, I. and Tossi, A. (2006) Cationic Antimicrobial Peptides-The Defensins. Handbook of Biologically Active Peptides. **Chapter 11**, 55-66
- 2 Schneider, J. J., Unholzer, A., Schaller, M., Schafer-Korting, M. and Korting, H. C. (2005) Human defensins. *J. Mol. Med.* **83**, 587-595
- 3 Ganz, T. and Lehrer, R. I. (1994) Defensins. *Curr Opin Immunol.* **6**, 584-589
- 4 Hoover, D. M., Rajashankar, K. R., Blumenthal, R., Puri, A., Oppenheim, J. J., Chertov, O. and Lubkowski, J. (2000) The structure of human beta-defensin-2 shows evidence of higher order oligomerization. *J. Biol. Chem.* **275**, 32911-32918
- 5 Hoover, D. M., Chertov, O. and Lubkowski, J. (2001) The structure of human beta-defensin-1: new insights into structural properties of beta-defensins. *J Biol Chem.* **276**, 39021-39026
- 6 Schibli, D. J., Hunter, H. N., Aseyev, V., Starner, T. D., Wiencek, J. M., McCray, P. B., Jr., Tack, B. F. and Vogel, H. J. (2002) The solution structures of the human beta-defensins lead to a better understanding of the potent bactericidal activity of HBD3 against *Staphylococcus aureus*. *J. Biol. Chem.* **277**, 8279-8289
- 7 Boniotto, M., Antcheva, N., Zelezetsky, I., Tossi, A., Palumbo, V., Verga Falzacappa, M. V., Sgubin, S., Braida, L., Amoroso, A. and Crovella, S. (2003) A study of host defence peptide beta-defensin 3 in primates. *Biochem. J.* **374**, 707-714
- 8 Tang, Y. Q. and Selsted, M. E. (1993) Characterization of the disulfide motif in BNBD-12, an antimicrobial beta-defensin peptide from bovine neutrophils. *J. Biol. Chem.* **268**, 6649-6653
- 9 Kluver, E., Adermann, K. and Schulz, A. (2006) Synthesis and structure-activity relationship of beta-defensins, multi-functional peptides of the immune system. *J. Pept. Sci.* **12**, 243-257
- 10 Ganz, T. (1999) Defensins and host defense. *Science.* **286**, 420-421
- 11 Yang, D., Biragyn, A., Kwak, L. W. and Oppenheim, J. J. (2002) Mammalian defensins in immunity: more than just microbicidal. *Trends Immunol.* **23**, 291-296
- 12 Pazgier, M., Hoover, D. M., Yang, D., Lu, W. and Lubkowski, J. (2006) Human beta-defensins. *Cell Mol. Life Sci.* **63**, 1294-1313

- 13 Yang, D., Chertov, O., Bykovskaia, S. N., Chen, Q., Buffo, M. J., Shogan, J., Anderson, M., Schroder, J. M., Wang, J. M., Howard, O. M. and Oppenheim, J. J. (1999) Beta-defensins: linking innate and adaptive immunity through dendritic and T cell CCR6. *Science*. **286**, 525-528
- 14 Pazgier, M., Li, X., Lu, W. and Lubkowski, J. (2007) Human defensins: synthesis and structural properties. *Curr. Pharm. Des.* **13**, 3096-3118
- 15 Crovella, S., Antcheva, N., Zelezetsky, I., Boniotto, M., Pacor, S., Verga Falzacappa, M. V. and Tossi, A. (2005) Primate beta-defensins--structure, function and evolution. *Curr. Protein Pept. Sci.* **6**, 7-21
- 16 Semple, C. A., Taylor, K., Eastwood, H., Barran, P. E. and Dorin, J. R. (2006) Beta-defensin evolution: selection complexity and clues for residues of functional importance. *Biochem. Soc. Trans.* **34**, 257-262
- 17 Mandal, M. and Nagaraj, R. (2002) Antibacterial activities and conformations of synthetic alpha-defensin HNP-1 and analogs with one, two and three disulfide bridges. *J. Pept. Res.* **59**, 95-104
- 18 Wu, Z., Hoover, D. M., Yang, D., Boulegue, C., Santamaria, F., Oppenheim, J. J., Lubkowski, J. and Lu, W. (2003) Engineering disulfide bridges to dissect antimicrobial and chemotactic activities of human beta-defensin 3. *Proc. Natl. Acad. Sci. U S A.* **100**, 8880-8885
- 19 Pazgier, M., Prah, A., Hoover, D. M. and Lubkowski, J. (2007) Studies of the biological properties of human beta-defensin 1. *J. Biol. Chem.* **282**, 1819-1829
- 20 Campopiano, D. J., Clarke, D. J., Polfer, N. C., Barran, P. E., Langley, R. J., Govan, J. R., Maxwell, A. and Dorin, J. R. (2004) Structure-activity relationships in defensin dimers: a novel link between beta-defensin tertiary structure and antimicrobial activity. *J. Biol. Chem.* **279**, 48671-48679
- 21 Kluver, E., Schulz-Maronde, S., Scheid, S., Meyer, B., Forssmann, W. G. and Adermann, K. (2005) Structure-activity relation of human beta-defensin 3: influence of disulfide bonds and cysteine substitution on antimicrobial activity and cytotoxicity. *Biochemistry.* **44**, 9804-9816
- 22 Krishnakumari, V., Singh, S. and Nagaraj, R. (2006) Antibacterial activities of synthetic peptides corresponding to the carboxy-terminal region of human beta-defensins 1-3. *Peptides.* **27**, 2607-2613
- 23 Tossi, A., Sandri, L. and Giangaspero, A. (2000) Amphipathic, alpha-helical antimicrobial peptides. *Biopolymers.* **55**, 4-30
- 24 Tossi, A., Sandri, L. and Giangaspero, A. (2002) New consensus hydrophobicity scale extended to non-proteinogenic amino acids. In *PEPTIDES 2002, Proceedings of the XXVII European Peptide Symposium* (Benedetti, E. and Pedone, C., eds.), pp. 416-417, Ziino, Naples, Italy
- 25 Zasloff, M. (1987) Magainins, a class of antimicrobial peptides from *Xenopus* skin: isolation, characterization of two active forms, and partial cDNA sequence of a precursor. *Proc. Natl. Acad. Sci. U S A.* **84**, 5449-5453
- 26 Tossi, A., Tarantino, C. and Romeo, D. (1997) Design of synthetic antimicrobial peptides based on sequence analogy and amphipathicity. *Eur. J. Biochem.* **250**, 549-558
- 27 Giangaspero, A., Sandri, L. and Tossi, A. (2001) Amphipathic alpha helical antimicrobial peptides. *Eur. J. Biochem.* **268**, 5589-5600

- 28 Zelezetsky, I. and Tossi, A. (2006) Alpha-helical antimicrobial peptides--using a sequence template to guide structure-activity relationship studies. *Biochim. Biophys. Acta.* **1758**, 1436-1449
- 29 Matsuzaki, K. (1998) Magainins as paradigm for the mode of action of pore forming polypeptides. *Biochim. Biophys. Acta.* **1376**, 391-400
- 30 Shai, Y. (2002) Mode of action of membrane active antimicrobial peptides. *Biopolymers.* **66**, 236-248
- 31 Huang, H. W. (2006) Molecular mechanism of antimicrobial peptides: the origin of cooperativity. *Biochim. Biophys. Acta.* **1758**, 1292-1302
- 32 Mozsolits, H., Wirth, H. J., Werkmeister, J. and Aguilar, M. I. (2001) Analysis of antimicrobial peptide interactions with hybrid bilayer membrane systems using surface plasmon resonance. *Biochim. Biophys. Acta.* **1512**, 64-76
- 33 Zelezetsky, I., Pacor, S., Pag, U., Papo, N., Shai, Y., Sahl, H. G. and Tossi, A. (2005) Controlled alteration of the shape and conformational stability of alpha-helical cell-lytic peptides: effect on mode of action and cell specificity. *Biochem. J.* **390**, 177-188
- 34 Pag, U., Oedenkoven, M., Sass, V., Shai, Y., Shamova, O., Antcheva, N., Tossi, A. and Sahl, H. G. (2008) Analysis of in vitro activities and modes of action of synthetic antimicrobial peptides derived from an alpha-helical "sequence template". *J. Antimicrob. Chemother.* **61**, 341-352
- 35 Ruhr, E. and Sahl, H. G. (1985) Mode of action of the peptide antibiotic nisin and influence on the membrane potential of whole cells and on cytoplasmic and artificial membrane vesicles. *Antimicrob. Agents Chemother.* **27**, 841-845
- 36 Zimmermann, G. R., Legault, P., Selsted, M. E. and Pardi, A. (1995) Solution structure of bovine neutrophil beta-defensin-12: the peptide fold of the beta-defensins is identical to that of the classical defensins. *Biochemistry.* **34**, 13663-13671
- 37 Circo, R., Skerlavaj, B., Gennaro, R., Amoroso, A. and Zanetti, M. (2002) Structural and functional characterization of hBD-1(Ser35), a peptide deduced from a DEFB1 polymorphism. *Biochem. Biophys. Res. Commun.* **293**, 586-592
- 38 Benincasa, M., Scocchi, M., Podda, E., Skerlavaj, B., Dolzani, L. and Gennaro, R. (2004) Antimicrobial activity of Bac7 fragments against drug-resistant clinical isolates. *Peptides.* **25**, 2055-2061
- 39 Sahly, H., Schubert, S., Harder, J., Rautenberg, P., Ullmann, U., Schroder, J. and Podschun, R. (2003) Burkholderia is highly resistant to human Beta-defensin 3. *Antimicrob. Agents Chemother.* **47**, 1739-1741
- 40 Pag, U., Oedenkoven, M., Papo, N., Oren, Z., Shai, Y. and Sahl, H. G. (2004) In vitro activity and mode of action of diastereomeric antimicrobial peptides against bacterial clinical isolates. *J. Antimicrob. Chemother.* **53**, 230-239
- 41 Antcheva, N., Boniotto, M., Zelezetsky, I., Pacor, S., Verga Falzacappa, M. V., Crovella, S. and Tossi, A. (2004) Effects of positively selected sequence variations in human and Macaca fascicularis beta-defensins 2 on antimicrobial activity. *Antimicrob. Agents Chemother.* **48**, 685-688

- 42 Del Pero, M., Boniotto, M., Zuccon, D., Cervella, P., Spano, A., Amoroso, A. and Crovella, S. (2002) Beta-defensin 1 gene variability among non-human primates. *Immunogenetics*. **53**, 907-913
- 43 Morgera, F., Antcheva, N., Pacor, S., Quaroni, L., Berti, F., Vaccari, L. and Tossi, A. (2008) Structuring and interactions of human beta-defensins 2 and 3 with model membranes. *J. Pept. Sci.* **14**, 518-523
- 44 Soruri, A., Grigat, J., Forssmann, U., Riggert, J. and Zwirner, J. (2007) beta-Defensins chemoattract macrophages and mast cells but not lymphocytes and dendritic cells: CCR6 is not involved. *Eur. J. Immunol.* **37**, 2474-2486
- 45 Sahl, H. G., Pag, U., Bonness, S., Wagner, S., Antcheva, N. and Tossi, A. (2005) Mammalian defensins: structures and mechanism of antibiotic activity. *J. Leukoc. Biol.* **77**, 466-475
- 46 Kluver, E., Schulz, A., Forssmann, W. G. and Adermann, K. (2002) Chemical synthesis of beta-defensins and LEAP-1/hepcidin. *J. Pept. Res.* **59**, 241-248
- 47 Bauer, F., Schweimer, K., Kluver, E., Conejo-Garcia, J. R., Forssmann, W. G., Rosch, P., Adermann, K. and Sticht, H. (2001) Structure determination of human and murine beta-defensins reveals structural conservation in the absence of significant sequence similarity. *Protein Sci.* **10**, 2470-2479
- 48 Sass, V., Pag, U., Tossi, A., Bierbaum, G. and Sahl, H. G. (2008) Mode of action of human beta-defensin 3 against *Staphylococcus aureus* and transcriptional analysis of responses to defensin challenge. *Int. J. Med. Microbiol.* **298**, 619-633
- 49 Maemoto, A., Qu, X., Rosengren, K. J., Tanabe, H., Henschen-Edman, A., Craik, D. J. and Ouellette, A. J. (2004) Functional analysis of the alpha-defensin disulfide array in mouse cryptdin-4. *J. Biol. Chem.* **279**, 44188-44196
- 50 Rohrl, J., Yang, D., Oppenheim, J. J. and Hehlhans, T. (2008) Identification and Biological Characterization of Mouse beta-defensin 14, the orthologue of human beta-defensin 3. *J. Biol. Chem.* **283**, 5414-5419
- 51 Taylor, K., Clarke, D. J., McCullough, B., Chin, W., Seo, E., Yang, D., Oppenheim, J., Uhrin, D., Govan, J. R., Campopiano, D. J., MacMillan, D., Barran, P. and Dorin, J. R. (2008) Analysis and separation of residues important for the chemoattractant and antimicrobial activities of beta-defensin 3. *J. Biol. Chem.* **283**, 6631-6639
- 52 Rotem, S., Radzishevsky, I. S., Bourdetsky, D., Navon-Venezia, S., Carmeli, Y. and Mor, A. (2008) Analogous oligo-acyl-lysines with distinct antibacterial mechanisms. *Faseb J.* **22**, 2652-2661

Accepted Manuscript

## FIGURE LEGENDS

### Figure 1 Comparative sequence analysis of $\beta$ -defensins

Qualitative representation of the positional variation, where larger histograms correlate with higher variability (A). Template indicating strongly (uppercase), moderately (lower case) and less conserved (x) positions (B). Template indicating most frequent residues or residue types at each position (x = highly variable, lower case > 30% frequency, uppercase > 60% frequency, H > 60% hydrophobic residues (C). Sequence of tBD (E is pyroglutamic acid) (D). Representation of  $\beta$ -defensin topology, based on known structures (grey arrows represent  $\beta$ -strands, the cylinder represents a possible  $\alpha$ -helical segment, it is shown as transparent as it is present in some family members but not others (E). Frequency plots for total charge and % hydrophobic residues for the analysed  $\beta$ -defensin sequences (F).

### Figure 2 Sequence alignment of tBD with selected natural $\beta$ -defensins

Residues identical to those in tBD are shaded grey. Sequences are named as in the UniProtKB database. The percent identity with tBD was calculated using the BLAST Network Service on ExPASy.

### Figure 3 Structure and aggregation

CD spectra of tBD compared to that of its analogues in 5mM SPB at pH 7 (A) or in the presence of 10 mM SDS micelles (B) with 20  $\mu$ M peptide concentration; tBD (—), tBD(Ser<sup>34</sup>) (····), tBD(10-38) (---), tBD (16-38) (----). Native SDS-PAGE in reducing (lanes 2, 4, 6, 8, 10, 12, 14) and non reducing conditions (lanes 3, 5, 7, 9, 11, 13, 15); lanes 1 and 16 are standards (C). For tBD(Ser<sup>34</sup>), fraction 1 was established by ESI-MS as being prevalently dimeric, while fraction 2 as prevalently monomeric, in non-reducing conditions (see supplementary Table S1).

### Figure 4 FTIR spectra of tBD and tBD(Ser<sup>34</sup>) in solution and in PG multilayers

Transmission FTIR spectra of 2 mM tBD (—) and tBD(Ser<sup>34</sup>) (····) in D<sub>2</sub>O after 24h H/D exchange (A) and ATR-FTIR spectra of tBD and tBD(Ser<sup>34</sup>) in PG multi-bilayers (peptide:lipid ratio 1:20 w/w) (B). The respective spectra second derivatives are shown in (C) and (D). The percentage undeuterated amide II band for tBD and tBD(Ser<sup>34</sup>) in PG multi-bilayers after 1, 4 and 12 h of H/D exchange (E).

### Figure 5 Dependence of the antimicrobial potency of tBD and its fragments on medium concentrations

MIC ( $\mu$ M) values for *Escherichia coli* ML-35 (A), for *Staphylococcus aureus* 710A (B) (in tryptic soy broth for both bacteria), and for *Candida albicans* c.i. in Sabouraud/dextrose medium. All micro-organism were tested at 10<sup>5</sup> CFU/ml; tBD (—◆—), tBD(10-38) (--■--) and tBD(16-38) (··▲··).

### Figure 6 Bacterial inactivation, membrane permeabilization kinetics and serum stability

Time killing plots for tBD (8  $\mu$ M) against *E. coli* ML-35 (—), control ( $\Delta$ ), tBD ( $\blacktriangle$ ) and *S. aureus* 710A (----), control ( $\circ$ ), tBD ( $\bullet$ ), (10<sup>7</sup> CFU/ml bacteria in SPB) (A). Membrane permeabilisation

assessed by following the kinetics of hydrolysis of extracellular ONPG substrate by cytoplasmic  $\beta$ -galactosidase (**B**); 10  $\mu$ M concentration of tBD (—), tBD(Ser<sup>34</sup>) (---), tBD(10-38) (....), tBD(16-38) (—·—). The membranolytic  $\alpha$ -helical peptide P19(5/B) (—·—) was used as positive control at 5  $\mu$ M concentration [28]. Stability of defensins in 25% (v/v) of untreated human serum in PBS; tBD (■), tBD(10-38) (▲), tBD(16-38) (△), hBD2 (○) and hBD3 (●) (**C**).

#### Figure 7 Mode of action of tBD on *S. simulans*

Time killing plot (**A**). Optical density at 600 nm taken in parallel with the colony count (**B**). Influence on the membrane potential, calculated using the Nernst equation, based on the distribution of the lipophilic cation TPP<sup>+</sup> inside and outside the cells (**C**). Accumulation of [<sup>3</sup>H]-L-glutamate into chloramphenicol-treated cells (**D**). Experiments were carried out in 25% (v/v) MH broth in the absence (··◆··) and presence of peptide (—■—) at 30  $\mu$ M (10 x MIC). In panel **D**, efflux of labelled amino acid (—●—) was measured also after addition of tBD to untreated cells, at the indicated time point (arrow).

#### Figure 8 Surface plasmon resonance sensograms for binding to model membranes

Panels **A & B** are sensograms for tBD, panels **C & D** for tBD(10-38) with neutral PC/Cholesterol (10/1 w/w, panels **A, C**) and anionic PE:PG (7:3 w/w, panels **B, D**) lipid bilayers, at increasing peptide concentrations of 0.45, 0.9, 1.8, 3.6, 7.0, 15, and 30  $\mu$ M. Panels **E & F** show the relationship between the peptide concentration and equilibrium binding response (RU<sub>eq</sub>), determined using the BIAcore's steady state affinity model. tBD (—●—), tBD(10-38) (—○—), and tBD(16-38) (—□—) with PC/Cholesterol (10/1 w/w, panel **E**) and PE:PG (7:3 w/w, panel **F**).

#### Figure 9 Effect of $\beta$ -defensins on immature dendritic cells

Cheomotaxis of iDC7 in the presence of hBD2, tBD and tBD(10-38) (1  $\mu$ M) or MIP-3 $\alpha$  (12.5 nM) used as positive control (black histogram). Values are expressed as chemotaxis index (induced/spontaneous, \*  $p < 0.05$ , values statistically different from spontaneous migration). Chemotaxis of cells treated with CCR6 neutralising antibody is shown as grey histograms (**A**). Percent apoptotic (subG1) cells (black histogram) and mitochondrial membrane depolarisation ( $\Delta\Psi_m$ ) (grey histogram) for iDC7 treated with 1  $\mu$ M peptide (\*  $p < 0.05$ , \*\*  $p < 0.01$ , values vs untreated control) (**B**). Statistical analysis was carried out using the Student-Newman-Keuls post test.

**Table 1 Primary structures and properties of template  $\beta$ -defensin tBD, its analog and fragments**

Peptide	Sequence	MW [Da]		Charge	AA	$\hat{H}^b$
		(calc)	(obs)			
	----- ----- ----- ----- ----- ----- 10      20      30					
tBD	 $\hat{E}GVSCLRNGGFCIPIRC\text{PGHTRQIGT}CFGPRVKCCRKW$	4212.1	4212.0	6	38	-1,75
tBD(Ser <sup>34</sup> )	 $\hat{E}GVSCLRNGGFCIPIRC\text{PGHTRQIGT}CFGPRVKS\text{CRKW}$	4198.0	4198.5	6	38	-1,78
tBD(10-38)	 $GCIPIRC\text{PGHTRQIGT}CFGPRVKS\text{CRKW}$	3300.9	3300.0	6	29	-1,52
tBD(16-38)	 $RC\text{PGHTRQIGT}SFGPRVKS\text{CRKW}$	2656.1	2655.5	6	23	-2,91
tBD(16-38)lin	 $RC\text{PGHTRQIGT}SFGPRVKS\text{CRKW}$	2772.1	2772.0	6	23	(<-3)

**a** - alkylated cystein residues ; <sup>b</sup> Mean per residue hydrophobicity calculated as per ref. (24);  $\hat{E}$  is pyroglutamic acid

**Table 2 Antimicrobial and hemolytic activity of tBD and its mutated or truncated analogues**

<sup>a</sup> MIC values were determined in 5 % (v/v) TSB for bacteria, and in 5 % (v/v) SAB medium for yeast, in 10 mM sodium phosphate buffer pH 7.4, using 10<sup>5</sup> CFU/ml micro-organisms at logarithmic phase, and are the mean of at least three experiments performed in duplicate.

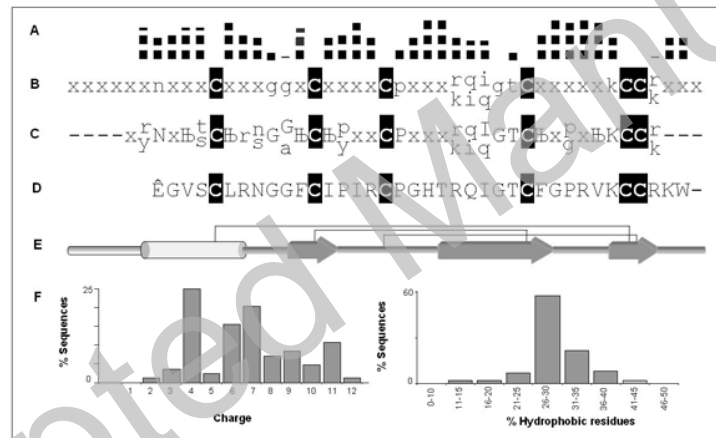
<sup>b</sup> The hemolytic activity of the peptides (10 or 100 µM) on erythrocytes was determined using 0.5% suspensions of human blood cells by monitoring the release of haemoglobin at 415 nm.

	Peptides					
	tBD	tBD(Ser <sup>34</sup> ) frac. 1	tBD(Ser <sup>34</sup> ) frac. 2	tBD(10-38)	tBD(16-38)	tBD(16-38) lin
	Antimicrobial activity (MIC, µM) <sup>a</sup>					
<i>E. coli</i>	2	2	4	1	2	8
<i>P. aeruginosa</i>	2-4	4	8	4	8	32
<i>S. aureus</i>	4	2	4	2	16	32
<i>C. albicans</i>	2	2	4	1	8	32
	Hemolytic activity (% lysis) <sup>b</sup>					
10 µM	10	30	nd	<10	<5	<5
100 µM	20	>90	nd	20	<5	<5

**Table 3 Comparison of the antimicrobial activity (MIC,  $\mu$ M) of tBD with selected human  $\beta$ -defensins and their primate orthologues**

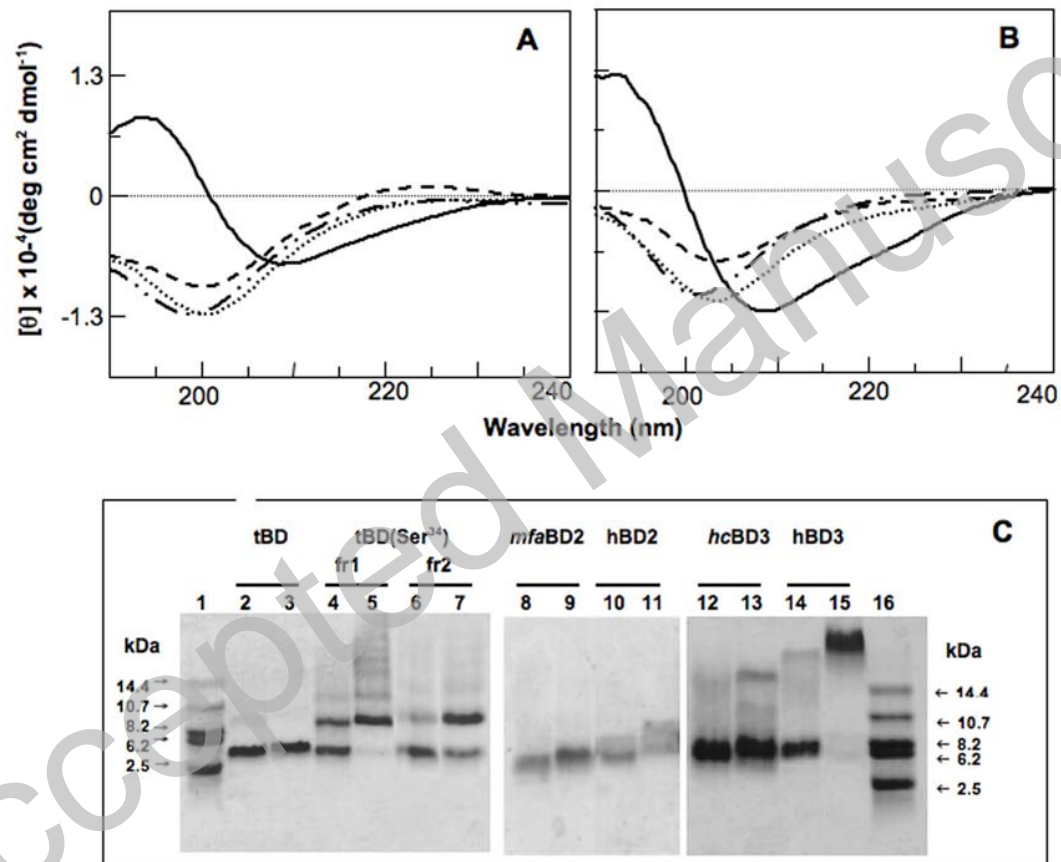
MIC values were determined in 5 % (v/v) TSB for bacteria or in 5 % (v/v) SAB medium for yeast in SPB using  $10^5$  CFU/ml micro-organisms at logarithmic phase, and are the mean of at least three experiments performed in duplicate.

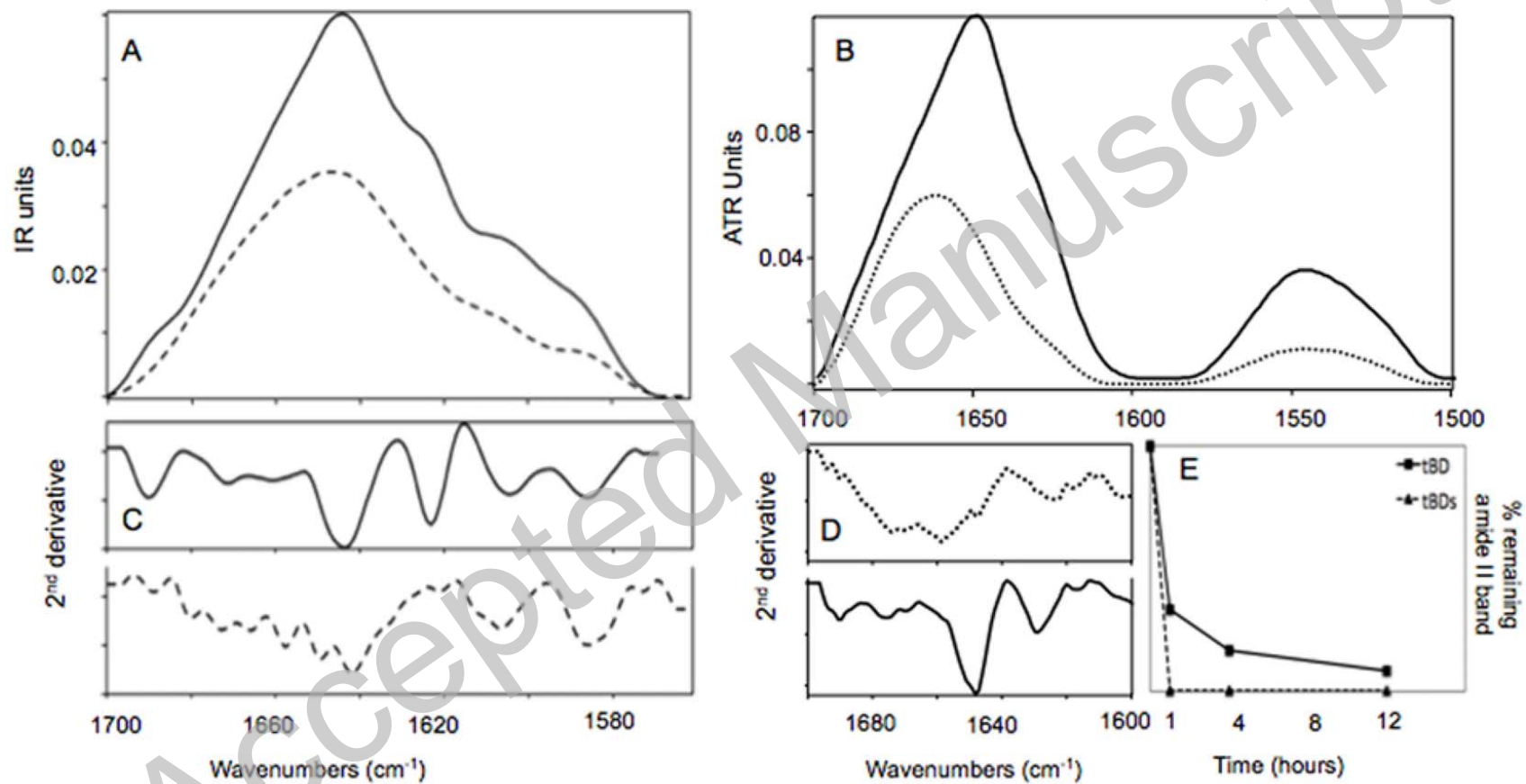
$\beta$ -defensin	Charge	<i>E. coli</i> ML35	<i>P. aeruginosa</i> ATCC 27853	<i>B. cepacia</i>		<i>S. aureus</i> 710A	<i>C. albicans</i> c.i.
				6981	14273		
tBD	+6	2	2-4	>32	>32	4	2
hBD1	+4	>32	>32	>32	>32	>32	>32
mfaBD1	+4	>32	>32	>32	>32	>32	8
hBD2	+6	4	4	>32	>32	8-16	16
mfaBD2	+7	4-8	8	>32	>32	4	4
hBD3	+11	1	2	>32	>32	1	2
hcBD3	+10	1	2	>32	>32	2	1

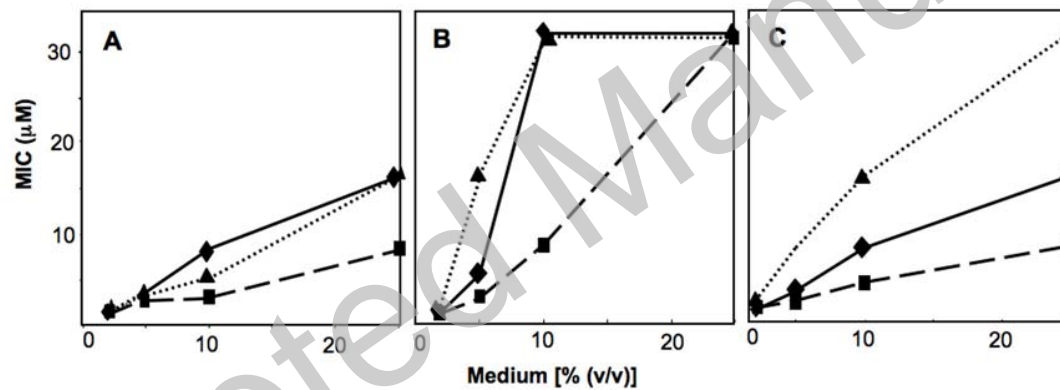


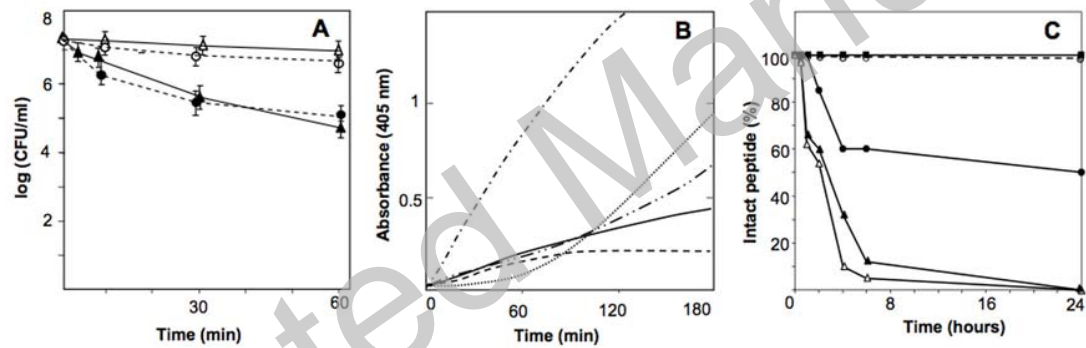
		10	20	30		Charge	Identity (%)
	-----	-----	-----	-----	-----		
tBD	----- <b>EGVS</b> CLRNGG <b>FC</b> IP <b>IR</b> CPGH <b>TR</b> Q <b>IGT</b> CFGPRV <b>K</b> CR <b>KW</b> ---					+6	
DEFB3_BOVIN	--- <b>EG</b> VRN <b>HVT</b> CRIN <b>RGF</b> CV <b>PI</b> RC <b>PG</b> R <b>TR</b> Q <b>IGT</b> CFG <b>PR</b> I <b>K</b> CR <b>RSW</b> ---					+9	79
DEFB13_BOVIN	---SGIS <b>GPLS</b> CG <b>R</b> NGG <b>V</b> CV <b>PI</b> RC <b>PV</b> PM <b>RQ</b> IG <b>T</b> CFG <b>R</b> P <b>VK</b> CR <b>RSW</b> ---					+6	79
DEFB1_SHEEP	---Q <b>G</b> V <b>RN</b> RL <b>S</b> CH <b>R</b> NG <b>V</b> CV <b>P</b> S <b>R</b> CP <b>R</b> H <b>M</b> R <b>Q</b> IG <b>T</b> CR <b>G</b> PP <b>VK</b> CR <b>RK</b> ---					+12	66
TAP_BOVIN	-----NP <b>V</b> S <b>C</b> VR <b>NK</b> GI <b>C</b> V <b>P</b> IR <b>C</b> PG <b>S</b> M <b>K</b> Q <b>IGT</b> CV <b>G</b> RA <b>VK</b> CR <b>RK</b> ---					+9	66
LAP_BOVIN	G <b>F</b> T <b>Q</b> G <b>V</b> R <b>N</b> S <b>Q</b> S <b>C</b> R <b>R</b> N <b>K</b> GI <b>C</b> V <b>P</b> IR <b>C</b> PG <b>S</b> M <b>R</b> Q <b>IGT</b> CL <b>G</b> A <b>Q</b> V <b>K</b> CR <b>RK</b> ---					+10	66
LAP_CAPHI	-----S <b>R</b> R <b>S</b> CH <b>R</b> NG <b>V</b> CA <b>L</b> T <b>R</b> CP <b>R</b> N <b>M</b> R <b>Q</b> IG <b>T</b> CF <b>G</b> PP <b>VK</b> CR <b>RK</b> ---					+11	63
DEFB1_PIG	----N <b>I</b> G <b>N</b> S <b>V</b> S <b>C</b> L <b>R</b> N <b>K</b> G <b>V</b> CM <b>P</b> G <b>K</b> CA <b>P</b> K <b>M</b> Q <b>IGT</b> CG <b>M</b> P <b>Q</b> V <b>K</b> CR <b>RK</b> ---					+9	53
DEFB1_HORSE	----G <b>I</b> E <b>T</b> S <b>F</b> S <b>C</b> S <b>Q</b> NG <b>G</b> F <b>C</b> L <b>S</b> P <b>K</b> CL <b>P</b> G <b>S</b> K <b>Q</b> IG <b>T</b> CI <b>L</b> P <b>G</b> S <b>K</b> CR <b>RK</b> ---					+5	53
DEFB3_MOUSE	---K <b>I</b> N <b>N</b> P <b>V</b> S <b>C</b> L <b>R</b> K <b>G</b> G <b>R</b> C <b>W</b> N <b>-P</b> I <b>V</b> N <b>T</b> R <b>Q</b> I <b>G</b> S <b>C</b> G <b>V</b> P <b>F</b> L <b>K</b> CR <b>RK</b> ---					+11	53
DEFB2_HUMAN	----G <b>I</b> G <b>D</b> P <b>V</b> T <b>CL</b> K <b>S</b> G <b>A</b> I <b>CH</b> P <b>V</b> F <b>CP</b> R <b>R</b> Y <b>K</b> Q <b>IGT</b> CG <b>L</b> P <b>G</b> T <b>K</b> CR <b>CK</b> K <b>P</b> ---					+6	50
DEFB2_MACFA	----D <b>I</b> R <b>N</b> P <b>V</b> T <b>CV</b> R <b>S</b> G <b>A</b> I <b>CL</b> P <b>G</b> F <b>CP</b> R <b>R</b> Y <b>K</b> H <b>I</b> G <b>V</b> CG <b>V</b> S <b>A</b> I <b>K</b> CR <b>CK</b> K <b>P</b> ---					+7	37
DEFB1_HUMAN	-----D <b>H</b> Y <b>N</b> CV <b>S</b> S <b>G</b> Q <b>CL</b> Y <b>S</b> A <b>CP</b> I <b>F</b> T <b>K</b> I <b>Q</b> G <b>T</b> CY <b>R</b> G <b>K</b> A <b>K</b> CR <b>CK</b> ----					+4	34
DEFB3_HUMAN	-G <b>I</b> I <b>N</b> T <b>L</b> Q <b>K</b> Y <b>Y</b> CR <b>V</b> R <b>G</b> G <b>R</b> CA <b>V</b> L <b>S</b> CL <b>P</b> K <b>E</b> E <b>Q</b> I <b>G</b> K <b>STR</b> G <b>R</b> K <b>CR</b> R <b>K</b> -					+11	34
DEFB3_HYLCO	-G <b>L</b> M <b>N</b> T <b>L</b> Q <b>K</b> Y <b>Y</b> CR <b>V</b> R <b>G</b> G <b>R</b> CA <b>V</b> L <b>S</b> CL <b>P</b> K <b>E</b> E <b>Q</b> I <b>G</b> K <b>STR</b> G <b>R</b> K <b>CR</b> R <b>K</b> -					+10	34
GLL1A_CHICK	-----G <b>R</b> K <b>S</b> D <b>CF</b> R <b>K</b> NG <b>F</b> CA <b>F</b> L <b>K</b> CP <b>Y</b> L <b>T</b> L <b>I</b> S <b>G</b> K <b>CSR</b> F <b>H</b> L <b>-C</b> CK <b>R</b> I <b>W</b> G					+8	32
DEFB4_HUMAN	----E <b>F</b> E <b>L</b> D <b>R</b> I <b>CG</b> Y <b>G</b> T <b>A</b> R <b>CR</b> K <b>-K</b> CR <b>S</b> Q <b>E</b> Y <b>R</b> I <b>G</b> R <b>CP</b> N <b>T</b> Y <b>A</b> -C <b>L</b> L <b>R</b> K <b>W</b> -					+7	21

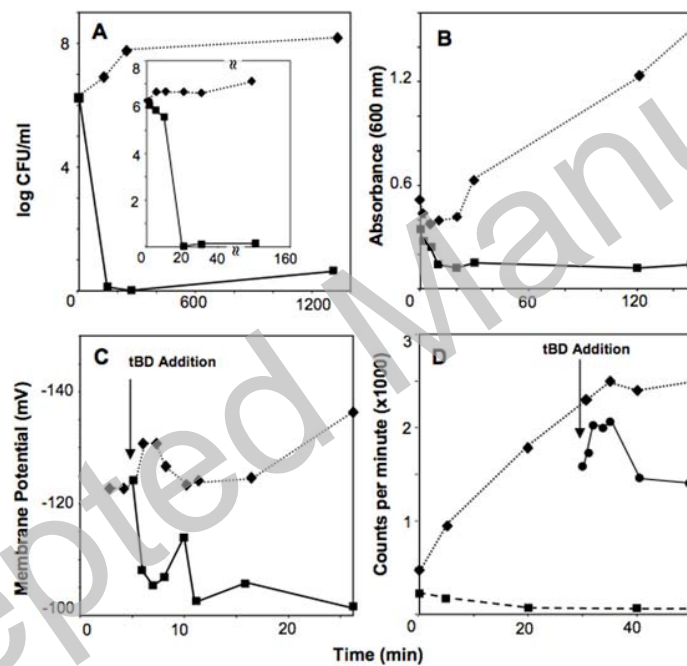
ACCEPTED MANUSCRIPT











THIS IS NOT THE VERSION OF RECORD - see doi:10.1042/BJ20082242

